Journal of Sound and Vibration 327 (2009) 134–143

Contents lists available at ScienceDirect

Journal of Sound and Vibration

journal homepage: www.elsevier.com/locate/jsvi

A study on the dynamics of rotating beams with functionally graded properties

M.T. Piovan [a,*], R. Sampaio [b]

[a] Centro de Investigaciones en Mecánica Teórica y Aplicada, Universidad Tecnológica Nacional, Facultad Regional Bahía Blanca, 11 de Abril 461, B8000LMI Bahía Blanca, BA, Argentina

[b] Department of Mechanical Engineering, Pontifícia Universidade Católica - Rio de Janeiro, Rua Marquês de São Vicente 225, Rio de Janeiro, RJ 22453-900, Brazil

ARTICLE INFO

Article history:
Received 2 December 2008
Accepted 16 June 2009
Handling Editor: C.L. Morfey
Available online 15 July 2009

ABSTRACT

The constant needs of the industry impel the engineering community in seeking of new concepts and new strategies in order to improve the structural response of structures as well as to enhance the endurance of materials. This is particularly true in the case of rotating blades that are subjected to severe environmental conditions such as high temperatures as well as mechanical conditions such as high rotating accelerations, centrifugal forces, geometric stiffening, among others. It is well known that flexible beams become stiffer when subjected to high speed rotations, because of the axial-bending coupling associated to the large displacements of the beam cross-section. This is called geometric stiffening effect and it was analyzed over the last decades in many beam applications from blade problems to drill-string modeling. In this paper a rotating nonlinear beam model accounting for arbitrary axial deformations is developed. The beam is made of functionally graded materials (FGM). This model is also employed to analyze other simplified models based on isotropic materials or composite materials, that are particular cases of the present formulation. The assumption of steady-state values of centrifugal loads is evaluated. It has to be said that there is a lack of information about modeling of beams made of functionally graded materials and this paper is intended to be a contribution on the subject.

1. Introduction

Strategic and high technology industries, such as defense, aerospace or automotive industries are demanding new and advanced materials in order to maintain or increase the leadership in the production of high competitive goods. Sometime ago, designers claimed for materials that combine in a unified fashion, the good properties of the metals and ceramics, that is, the stiffness, electrical conductivity and machinability of metals and the high strength, low density and high temperature resistance of ceramics. During the past 10 or 12 years these kinds of advanced materials are becoming no longer experimental specimens in laboratories but a well-developed reality. Functionally graded materials (FGM) are just an example of such advanced materials. The variation in percentage of the material constituents can be arranged in such a way to create a new material with graded properties in spatial directions. It is well known that one of the consequences of an interface is the appearance of gradients, of temperature and stress, and that the use of functionally graded materials precludes the appearance of this gradients.

* Corresponding author. Tel.: +54 291 4555 220; fax: +54 291 4555 311.
E-mail address: mpiovan@frbb.utn.edu.ar (M.T. Piovan).

0022-460X/$ - see front matter © 2009 Elsevier Ltd. All rights reserved.
doi:10.1016/j.jsv.2009.06.015

There are a number of papers dealing with general mechanics of beams, shells and plates made of functionally graded materials. In the particular case of functionally graded beams the works of Sankar [1], Chakraborty et al. [2] and Kapuria et al. [3], among others, offer interesting features, applications and calculation methodologies. These models are developed by means of different constitutive hypotheses (graded metallic-ceramic, graded multilayered, etc.) and displacement formulation (i.e. elementary Bernoulli–Euler or Timoshenko or higher order shear-deformable theories). The constitutive modeling is commonly related to a classical rule of mixtures and the material properties may vary according to a power law expression [2] or an exponential expression [1].

Rotating beams play an important role in the modeling of engineering applications such as turbine blades, airplane propellers and robot manipulators among others. This subject has been investigated with different level of intensity, at least, over the last four decades. Interesting reviews about rotating beams can be found in papers given by Rao [4] and Chung and Yoo [5]. In these papers one can find many epoch-making and very recent investigations about rotating beams made of isotropic metallic materials and even composite materials. Simo and Vu-Quoc [6,7] showed that the appropriate consideration of nonlinear strain–displacement relationships plays an important role in the correct modeling of the geometric stiffening of flexible beams. It is important to mention that the geometric stiffening has a remarkable effect in the dynamics of rotating and non-rotating beams. Moreover in rotating beams the geometric stiffening is not only due to certain strain–displacement expression but also due to centrifugal and Coriolis' effects as well. Now, taking into account the technological context, it is important to mention that there is a lack of information about rotating beams constructed with functionally graded materials. Thus, to the best of the authors knowledge, the papers of Fazelzadeh et al. [8] and Fazelzadeh and Hosseini [9] are the first ones dealing with rotating beams made of functionally graded materials. However, in these formulations the geometrical stiffness was not taken into account. The interest of these papers was focused in the thermoelastic effects related to graded properties.

In the following sections, a nonlinear model is developed appealing to a nonlinear strain–displacement relation. The model is derived through a common variational principle. The model is based on a formulation that includes shear deformation, that is a Timoshenko-like beam structure. The thermal effects are neglected at this stage because the main interest of the paper is the study of the influence of the graded properties in the damping effects and geometric stiffening of the rotating beam. The finite element method is employed to discretize the model and to obtain a numerical approximation of the motion equations. The interpolation functions allow the integration of the element matrices in a consistent form. Thus, the element can be used to calculate the response of a Bernoulli–Euler beam (as a limiting case) avoiding the shear locking phenomenon. Comparisons between the nonlinear model and its linearization are carried out. Parametric studies considering different slenderness ratios, different material constituents and motion patterns are performed as well.

2. Beam model formulation

In Fig. 1 one can see a sketch of a rotating beam undergoing arbitrary in-plane rotations, where $O:xyz$ and $O:XYZ$ are the rotating and inertial frames, respectively. The rotation of the beam is characterized by means of a prescribed rotation $\psi(t)$ around the z-axis. The cross-section is rectangular and composed of a metallic core and ceramic surfaces as shown in Fig. 2. The functionally graded beam is considered to be composed of isotropic homogeneous layers [10]. Then, graded properties of the beam can vary according to the following expression:

$$\mathscr{P}(z) = \mathscr{P}_m + (\mathscr{P}_c - \mathscr{P}_m)\left|\frac{2z}{h}\right|^n, \tag{1}$$

where $\mathscr{P}(z)$ denotes a typical material property (i.e. density or Young's modulus E or shear elastic modulus G, among others), $\mathscr{P}_m$ and $\mathscr{P}_c$ intend for metallic and ceramic properties. The exponent n is a variable such that $n \geq 0$; its magnitude gives the variation form of the properties as one can see in Fig. 2. It has to be mentioned that in the literature of structures constructed with functionally graded materials, the most common specimen is ceramic-rich in one surface (at $z = h/2$) and metallic-rich at the parallel surface (at $z = -h/2$). On the contrary, in this paper the beam has ceramic-rich properties at both surfaces, protecting a metallic core as shown in Fig. 2.

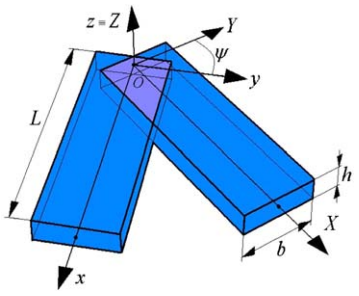

Fig. 1. Reference frames of the rotating beam.

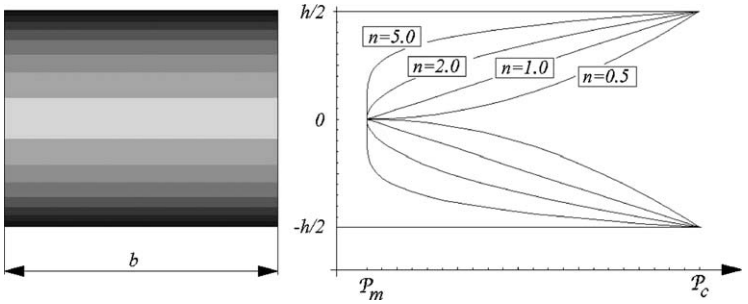

Fig. 2. Examples of graded properties, $\mathscr{P}(z)$.

For a beam rotating around the z-axis, the position vector of a generic point $(\bar{p})(p_x, p_y)$ may be written as

$$\bar{p} = \begin{Bmatrix} p_x \\ p_y \end{Bmatrix} = \begin{bmatrix} \mathrm{Cos}[\psi] & -\mathrm{Sin}[\psi] \\ \mathrm{Sin}[\psi] & \mathrm{Cos}[\psi] \end{bmatrix} \begin{Bmatrix} u_x + x \\ u_y + y \end{Bmatrix}, \tag{2}$$

where u_x and u_y are the displacements of a generic point of the deformed configuration measured with respect to the rotating frame:

$$u_x(x, y, t) = u(x, t) - y\theta(x, t),$$

$$u_y(x, y, t) = v(x, t). \tag{3}$$

The variables u, v and θ are the extensional displacement, lateral displacement and bending rotation of the cross-section, respectively. As one can easily see, Eq. (3) is describing a typical shear-deformable or Timoshenko formulation.

Taking into account the definition of the Lagrangian strain tensor and Eq. (3), one can obtain the in-plane components of the strain tensor as

$$\varepsilon_{xx} = u' - y\theta' + \tfrac{1}{2}[(u' - y\theta')^2 + v'^2],$$

$$\gamma_{xy} = (v' - \theta) + [-\theta(u' - y\theta')]. \tag{4}$$

The velocity vector of a generic point can be obtained from (2) in the following form:

$$\dot{\bar{p}} = \begin{Bmatrix} -[(u + x - y\theta)\dot{\psi} + \dot{v}]\mathrm{Sin}[\psi] - [(v + y)\dot{\psi} - (\dot{u} - y\dot{\theta})]\mathrm{Cos}[\psi] \\ -[(v + y)\dot{\psi} - (\dot{u} - y\dot{\theta})]\mathrm{Sin}[\psi] + [(u + x - y\theta)\dot{\psi} + \dot{v}]\mathrm{Cos}[\psi] \end{Bmatrix}. \tag{5}$$

In Eqs. (4), (5) and in the following paragraphs, dots and apostrophes identify derivatives with respect to time and space (i.e. x), respectively.

Now the strain energy and the kinetic energy of a functionally graded rotating beam can be defined as

$$U_D = \frac{1}{2}\int_V [E(z)\varepsilon_{xx}^2 + kG(z)\gamma_{xy}^2]\,\mathrm{d}V,$$

$$U_K = \frac{1}{2}\int_V [\rho(z)\dot{\bar{p}} \cdot \dot{\bar{p}}]\,\mathrm{d}V, \tag{6}$$

where $E(z)$, $G(z)$ and $\rho(z)$ are Young's modulus, shear modulus and density, respectively; whereas k is the Timoshenko shear coefficient.

In this paper the shear coefficient is taken, as an approximation, equal to the isotropic case, i.e. $k = \frac{5}{6}$. Now, substituting Eqs. (4) and (5) into Eq. (6), one obtains

$$\begin{aligned} U_D = {} & \frac{1}{2}\int_L [J_{11}^E u'^2 + J_{22}^E \theta'^2 + J_{11}^G (v' - \theta)^2]\,\mathrm{d}x \\ & + \frac{1}{2}\int_L \underline{[J_{11}^E (u'^3 + u'v'^2) + 3J_{22}^E u'\theta'^2 - 2J_{11}^G (v' - \theta)u'\theta]\,\mathrm{d}x} \\ & + \frac{1}{2}\int_L \underline{\underline{\left[J_{11}^E \left(\frac{1}{4}u'^4 + \frac{1}{2}u'^2v'^2 + \frac{1}{4}v'^4\right) + J_{22}^E \left(\frac{3}{2}u'^2 + \frac{1}{2}v'^2\right)\theta'^2\right]\,\mathrm{d}x}} \\ & + \frac{1}{2}\int_L \underline{\underline{\left[\frac{1}{4}J_{33}^E \theta'^4 + J_{11}^G \left(u'^2\theta'^2\right) + J_{22}^G \left(\theta^2\theta'^2\right)\right]\mathrm{d}x}}, \end{aligned} \tag{7}$$

$$U_K = \frac{1}{2}\int_L J_{11}^{\rho}[\dot{u}^2 + \dot{v}^2 + 2\dot{\psi}(\dot{v}(u+x) - \dot{u}v)]\,\mathrm{d}x + \frac{1}{2}\int_L J_{11}^{\rho}[\dot{\psi}^2(u^2 + v^2 + 2ux + x^2)]\,\mathrm{d}x + \frac{1}{2}\int_L J_{22}^{\rho}[\dot{\theta}^2 + 2\dot{\theta}\dot{\psi} + (1+\theta^2)\dot{\psi}^2]\,\mathrm{d}x, \tag{8}$$

where

$$\{J_{ij}^E, J_{ij}^G, J_{ij}^{\rho}\} = \int_A \{E(z), kG(z), \rho(z)\}(\bar{g}_i \cdot \bar{g}_j)\,\mathrm{d}y\,\mathrm{d}z, \quad \forall \bar{g} = \{1, y, y^2\}. \tag{9}$$

The nonlinear equations of motion can be derived by means of Hamilton's principle, i.e.:

$$\delta \int_{t_1}^{t_2} (U_K - U_{DR})\,\mathrm{d}t = 0, \tag{10}$$

where U_{DR} is the reduced strain energy derived from Eq. (7) in which the double underlined terms are assumed negligible as in many papers of rotating beam made of isotropic materials [10]. This approach is also considered in the study of geometric stiffening effect of non-rotating beams [11]. It is noticeable that the elimination of every underlined term in Eq. (7), leads to a linear formulation.

3. Finite element approach

Finite element models can be constructed through discretization of the Hamilton principle expression (10). The discretization is carried out using Lagrange linear shape functions for axial displacements, cubic shape functions for the lateral displacement, and quadratic shape functions for bending rotation. That is:

$$u = \mathbf{N}_u \mathbf{q}_e,$$

$$v = \mathbf{N}_v \mathbf{q}_e,$$

$$\theta = \mathbf{N}_\theta \mathbf{q}_e, \tag{11}$$

where

$$\mathbf{q}_e = \{u_1, v_1, \theta_1, u_2, v_2, \theta_2\}^T,$$

$$\mathbf{N}_u = \{1-\xi, 0, 0, \xi, 0, 0\},$$

$$\mathbf{N}_v = \left\{0, \frac{1+\beta(1-\xi) - 3\xi^2 + 2\xi^3}{1+\beta}, \frac{[2+\beta-(4+\beta)\xi + 2\xi^2]\xi L_e}{2(1+\beta)}, 0, \frac{\beta\xi + 3\xi^2 - 2\xi^3}{1+\beta}, \frac{[-\beta + (\beta-2)\xi + 2\xi^2]\xi L_e}{2(1+\beta)}\right\},$$

$$\mathbf{N}_\theta = \left\{0, \frac{6\xi(\xi-1)}{L_e(1+\beta)}, \frac{[1+\beta-(4+\beta)\xi + 3\xi^2]}{1+\beta}, 0, -\frac{6\xi(\xi-1)}{L_e(1+\beta)}, \frac{(-2+\beta+3\xi)\xi}{1+\beta}\right\}, \tag{12}$$

L_e is the length of the generic element, ξ and β are such that

$$\xi = \frac{x}{L_e}, \quad \beta = \frac{12 J_{22}^E}{L_e^2 J_{11}^G}. \tag{13}$$

The interpolating functions summarized in Eq. (12) give a consistent integration of the equations of a shear-deformable isotropic beam as one can see in Refs. [12,13]. Moreover $\mathbf{N}_v$ and $\mathbf{N}_\theta$ can also be employed to approximate the solution of a Bernoulli–Euler beam equation because when $\beta \to 0$ (or in other words $J_{11}^G \to \infty$, i.e. the non-shear-deformable hypothesis), and the interpolating functions reduce to cubic and quadratic Hermite's polynomials.

Now, substituting Eq. (12) in Eq. (13) and then in Eqs. (7) and (8), after performing the conventional steps of variational calculus in Eq. (10) one gets the equation for a single finite element in the following form:

$$\mathbf{M}_e \ddot{\mathbf{q}}_e - 2\dot{\psi}\mathbf{G}_e\dot{\mathbf{q}}_e + [\mathbf{K}_e + \mathbf{K}_{ge}(\mathbf{q}_e) - \dot{\psi}^2\mathbf{M}_e - \ddot{\psi}\mathbf{G}_e]\mathbf{q}_e = \dot{\psi}^2\mathbf{f}_A - \ddot{\psi}\mathbf{f}_T, \tag{14}$$

where

$$\mathbf{M}_e = \int_0^1 [J_{11}^{\rho}(\mathbf{N}_u^T\mathbf{N}_u + \mathbf{N}_v^T\mathbf{N}_v) + J_{22}^{\rho}\mathbf{N}_\theta^T\mathbf{N}_\theta]L_e\,\mathrm{d}\xi, \tag{15}$$

$$\mathbf{G}_e = \int_0^1 [J_{11}^{\rho}(\mathbf{N}_u^T\mathbf{N}_v - \mathbf{N}_v^T\mathbf{N}_u)]L_e\,\mathrm{d}\xi, \tag{16}$$

$$\mathbf{K}_e = \int_0^1 [J_{11}^E \mathbf{N}_u'^T \mathbf{N}_u' + J_{22}^E \mathbf{N}_\theta'^T \mathbf{N}_\theta'] \frac{1}{L_e}\,\mathrm{d}\xi + \int_0^1 [J_{11}^G (\mathbf{N}_\nu'^T - L_e \mathbf{N}_\theta^T)(\mathbf{N}_\nu' - L_e \mathbf{N}_\theta)] \frac{1}{L_e}\,\mathrm{d}\xi, \tag{17}$$

$$\begin{aligned}\mathbf{K}_{ge} = & \int_0^1 \frac{J_{11}^E}{2L_e^2} [3\mathbf{N}_u'^T \mathbf{N}_u' \mathbf{q}_e \mathbf{N}_u' + \mathbf{N}_u'^T \mathbf{N}_\nu' \mathbf{q}_e \mathbf{N}_\nu']\,\mathrm{d}\xi + \int_0^1 \frac{J_{11}^E}{2L_e^2} [\mathbf{N}_\nu'^T \mathbf{N}_u' \mathbf{q}_e \mathbf{N}_\nu' + \mathbf{N}_\nu'^T \mathbf{N}_\nu' \mathbf{q}_e \mathbf{N}_u']\,\mathrm{d}\xi \\ & + \int_0^1 \frac{3J_{22}^E}{2L_e^2} [\mathbf{N}_u'^T \mathbf{N}_\theta' \mathbf{q}_e \mathbf{N}_\theta' + \mathbf{N}_\theta'^T \mathbf{N}_u' \mathbf{q}_e \mathbf{N}_\theta' + \mathbf{N}_\theta'^T \mathbf{N}_\theta' \mathbf{q}_e \mathbf{N}_u']\,\mathrm{d}\xi \\ & - \int_0^1 \frac{J_{11}^G}{2L_e} [\mathbf{N}_u'^T \mathbf{N}_\theta \mathbf{q}_e (\mathbf{N}_\nu' - L_e \mathbf{N}_\theta) + \mathbf{N}_u'^T (\mathbf{N}_\nu' - L_e \mathbf{N}_\theta) \mathbf{q}_e \mathbf{N}_\theta]\,\mathrm{d}\xi \\ & - \int_0^1 \frac{J_{11}^G}{2L_e} [\mathbf{N}_\theta^T \mathbf{N}_u' \mathbf{q}_e (\mathbf{N}_\nu' - L_e \mathbf{N}_\theta) + \mathbf{N}_\theta^T (\mathbf{N}_\nu' - L_e \mathbf{N}_\theta) q_e \mathbf{N}_u']\,\mathrm{d}\xi \\ & - \int_0^1 \frac{J_{11}^G}{2L_e} [(\mathbf{N}_\nu'^T - L_e \mathbf{N}_\theta^T) \mathbf{N}_\theta \mathbf{q}_e \mathbf{N}_u' + (\mathbf{N}_\nu'^T - L_e \mathbf{N}_\theta^T) \mathbf{N}_u' \mathbf{q}_e \mathbf{N}_\theta]\,\mathrm{d}\xi, \end{aligned} \tag{18}$$

$$\mathbf{f}_A = \int_0^1 [J_{11}^\rho \mathbf{N}_u^T L_e \xi] L_e\,\mathrm{d}\xi, \tag{19}$$

$$\mathbf{f}_T = \int_0^1 [J_{11}^\rho \mathbf{N}_\nu^T L_e \xi + J_{22}^\rho \mathbf{N}_\theta^T] L_e\,\mathrm{d}\xi. \tag{20}$$

After the assembling process one gets the following expression:

$$\mathbf{M}\ddot{\mathbf{Q}} + \mathbf{C}\dot{\mathbf{Q}} + [\mathbf{K} + \mathbf{K}_G(\mathbf{Q}) + \mathbf{K}_D]\mathbf{Q} = \mathbf{F}, \tag{21}$$

where $\mathbf{M}$ is the global mass matrix, $\mathbf{C}$ is the global gyroscopic matrix, $\mathbf{K}$ is the global elastic stiffness matrix, $\mathbf{K}_G$ is the global geometric stiffness matrix, $\mathbf{K}_D$ corresponds to the stiffness induced by the rotation of the beam and $\mathbf{F}$ is the global vector of dynamical forces. One may notice that $\mathbf{K}_D$ is not symmetric due to the presence of the term proportional to the rotating acceleration $\ddot{\psi}$.

The matrix $\mathbf{C}$ can be modified in order to account for "a posteriori" structural damping, i.e.:

$$\mathbf{C} = \mathbf{G} + \mathbf{C}_{\mathrm{RD}}. \tag{22}$$

The matrix $\mathbf{G}$ is the global gyroscopic matrix and the matrix $\mathbf{C}_{\mathrm{RD}}$ corresponds to the system proportional Rayleigh damping given by

$$\mathbf{C}_{\mathrm{RD}} = \alpha\mathbf{M} + \eta\mathbf{K}. \tag{23}$$

The coefficients α and η in Eq. (23) can be computed from two experimental modal damping coefficients (namely, ξ_1 and ξ_2) for the first and second frequencies according to the common methodology presented bibliography related to finite element procedures [14] and vibration analysis [15]. Remember that $\mathbf{M}$ is the global mass matrix and $\mathbf{K}$ is the global elastic stiffness matrix. The Matlab odesuite is employed to simulate numerically the finite element model, for this reason Eq. (21) is represented in the following form:

$$\mathbf{A}\frac{\mathrm{d}\mathbf{W}}{\mathrm{d}t} + \mathbf{B}\mathbf{W} = \mathbf{D}, \tag{24}$$

where

$$\mathbf{A} = \begin{bmatrix} \mathbf{C} & \mathbf{M} \\ \mathbf{M} & \mathbf{0} \end{bmatrix}, \quad \mathbf{B} = \begin{bmatrix} \mathbf{K} + \mathbf{K}_G(\mathbf{Q}) + \mathbf{K}_D & \mathbf{0} \\ \mathbf{0} & -\mathbf{M} \end{bmatrix}, \tag{25}$$

$$\mathbf{W} = \left\{ \mathbf{Q}, \frac{\mathrm{d}\mathbf{Q}}{\mathrm{d}t} \right\}^{\mathrm{T}}, \quad \mathbf{D} = \begin{Bmatrix} \mathbf{F} \\ \mathbf{0} \end{Bmatrix}. \tag{26}$$

4. Numerical studies

In the present section a numerical testing of the procedure as well as parametric studies are performed in order to establish the validity and usefulness of the finite element approach. The first examples consist of comparisons of the finite element procedure with previous models that are contained in the present theory as limit cases. From Eq. (1) one can easily see that in the case of a homogeneous isotropic material, $\mathscr{P}_m = \mathscr{P}_c$, then there is no variation of properties. Thus, in Table 1 one can see the first three natural frequencies of a very slender metallic beam. The analytical solution of a classic model and experimental data [16] are compared with the present finite element approach. The beam is constructed with steel (see Table 2 for material properties) and its geometrical properties are such that $h = 22.12$ mm, $b = 2.66$ mm, $L = 152.40$ mm.

Table 1
Comparison of natural frequencies of a metallic cantilever beam (Hz).

Present approach FEM	Ref. [16] Analytical	Ref. [16] Experimental
97.0	96.9	97.0
607.5	607.6	610.0
1697.0	1699.0	1693.0

Table 2
Properties of metallic and ceramic materials.

Properties of materials	Steel	Aluminium	Alumina (Al_2O_3)
Young's modulus E [GPa]	214.00	79.80	390.00
Shear modulus G [GPa]	82.20	49.70	137.00
Material density ρ [kg/m^3]	7800.00	2690.00	3200.00

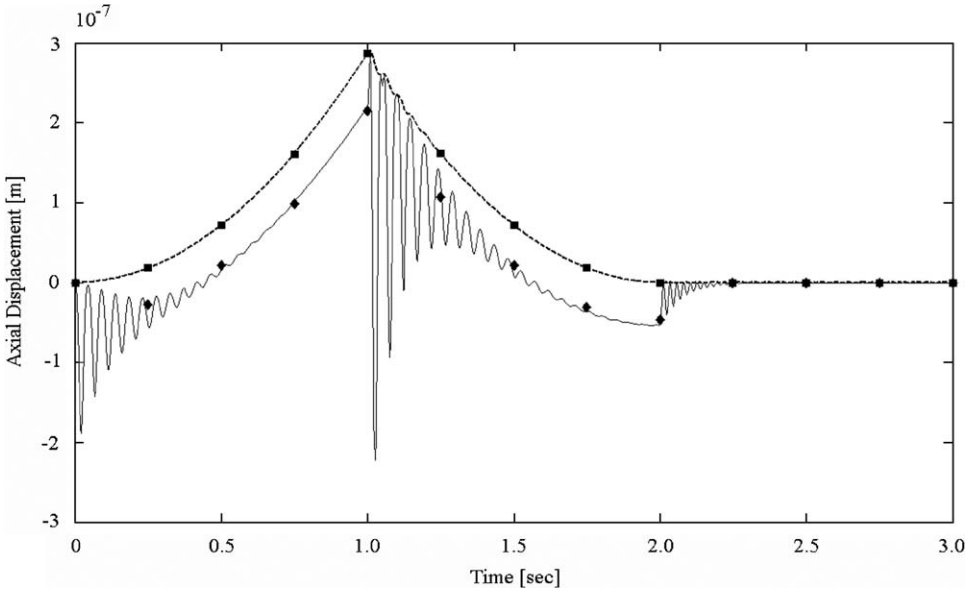

Fig. 3. Comparison of the present theory with previous approaches. Dotted line: present linear approach; continuous line: present nonlinear approach; (■) linear model [10]; (◆) nonlinear model [10].

The beam does not rotate and it is clamped at $x = 0$ and free at $x = L$. The frequencies have been calculated with a model of 10 finite elements that gave percentage differences lower that 0.5 percent with the analytical and experimental counterparts.

The second example is a comparison of present rotating beam model with the model developed by Trindade and Sampaio [10]. These authors developed a model for a metallic rotating beam under the context of Bernoulli–Euler hypotheses. As it is mentioned above the present shear-deformable model can be reduced to the case of a Bernoulli–Euler metallic beam by neglecting the terms associated with shear deformations (this may be done through the finite element procedure, i.e. Eq. (12) with $\beta = 0$) and imposing the condition $\mathscr{P}_m = \mathscr{P}_c$ in Eq. (1). The rotating beam is made of aluminium (see Table 2 for properties) and the geometrical properties are such that $h = 25$ mm, $b = 4$ mm and $L = 400$ mm. The damping properties are such that the damping coefficient for the first and second frequencies were taken as $\xi_1 = 0.01$ and $\xi_2 = 0.01$ (see Ref. [14] for the methodology). The beam rotates with the following rule given in Eq. (27). Five finite elements were employed to integrate numerically (by means of Matlab function "ode15s") the equations of motion:

$$\dot{\psi}(t) = \begin{cases} 50t, & \forall t \in [0,1), \\ 50(2-t), & \forall t \in [1,2], \\ 0, & \forall t > 2. \end{cases} \tag{27}$$

In Fig. 3 the axial displacements calculated for both linear and nonlinear approaches are shown. The responses of the present model and the beam developed in Ref. [10] are compared as well. One can see a good correlation (it has to be mentioned that the data for comparison purposes were taken from a figure).

The third example corresponds to an analysis of the variation of natural frequencies of a non-rotating functionally graded cantilever beam with respect to the exponent n of Eq. (1). The beam has a length $L = 1$ m and a cross-section with dimensions $b = 0.02$ m and $h = 0.01$ m. The metallic constituent is steel and the ceramic constituent is alumina, Al_2O_3, whose properties are summarized in Table 2. In Fig. 4, one can see the variation of the first three natural frequencies of a functionally graded beam with respect to the exponent n. Notice that the three frequencies vary monotonically from the highest value corresponding to the case in which the beam is made of ceramic material (i.e. $n = 0$) to the case in which the beam is made of steel (i.e. $n \to \infty$). Note that according to Eq. (1), when $n = 8$ the metallic constituent occupies nearly 90 percent of the beam volume. In this calculation, models with 10 finite elements were employed.

The last example corresponds to a functionally graded beam that rotates with the rule defined in Eq. (27). The geometrical properties of the beam are: $L = 1$ m, $b = 0.02$ m and $h = 0.01$ m. The material properties vary from a steel core to ceramic surfaces of alumina; see Table 2 for material properties. For simulation purposes the damping coefficients are assumed to be $\xi_1 = 0.002$ and $\xi_2 = 0.002$. Figs. 5 and 6 show the lateral deflection of the beam tip during a 3 s period for beams having $n = 0.4$ and 2.0, respectively, or in other words a beam rich in ceramic constituent ($n = 0.4$) and a beam rich in steel constituent ($n = 2.0$). The linear and nonlinear models derived from the present formulation are compared.

The dynamic behavior can be divided into three parts according to Eq. (27). Thus the instantaneous acceleration (at $t = 0$ s) and counter-acceleration (at $t = 1$ s) of the base leads to transient lateral vibrations which are slightly damped after a period of 0.4 s from the change of motion. For a ceramic-rich beam, during the positive and negative acceleration processes the linear and nonlinear models, in appearance, have the same deflections as one can see in Fig. 5. However, the

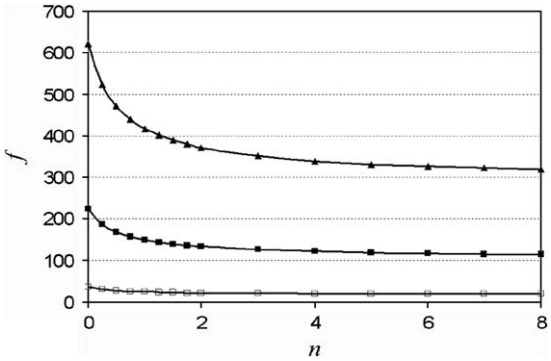

Fig. 4. Variation of the natural frequencies (f in [Hz]) of a functionally graded beam. (□) first frequency, (■) second frequency, (▲) third frequency.

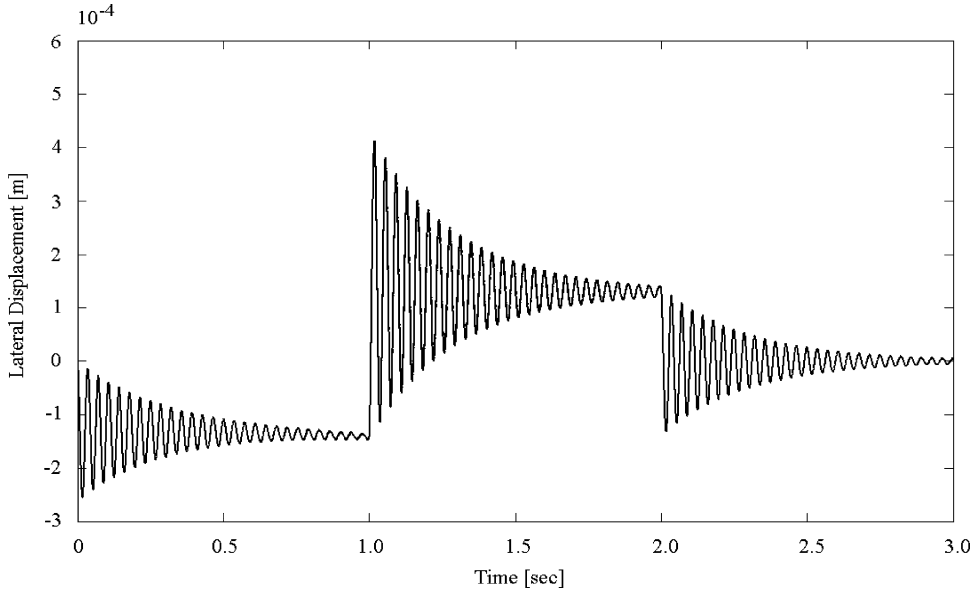

Fig. 5. Lateral displacement for a beam rich in ceramic constituent, dotted line for linear approach and continuous line for nonlinear approach.

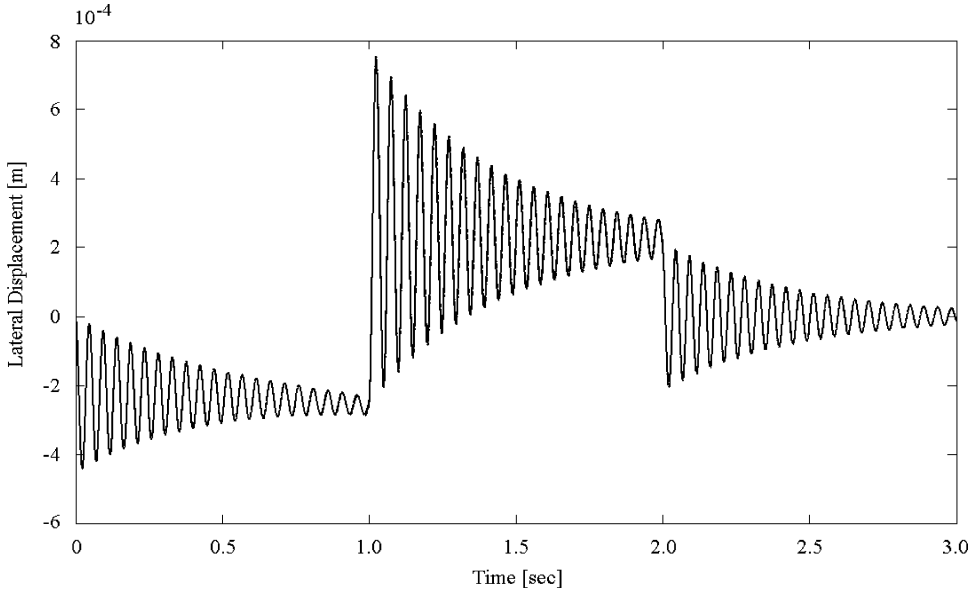

Fig. 6. Lateral displacement for a beam rich in metallic constituent, dotted line for linear approach and continuous line for nonlinear approach.

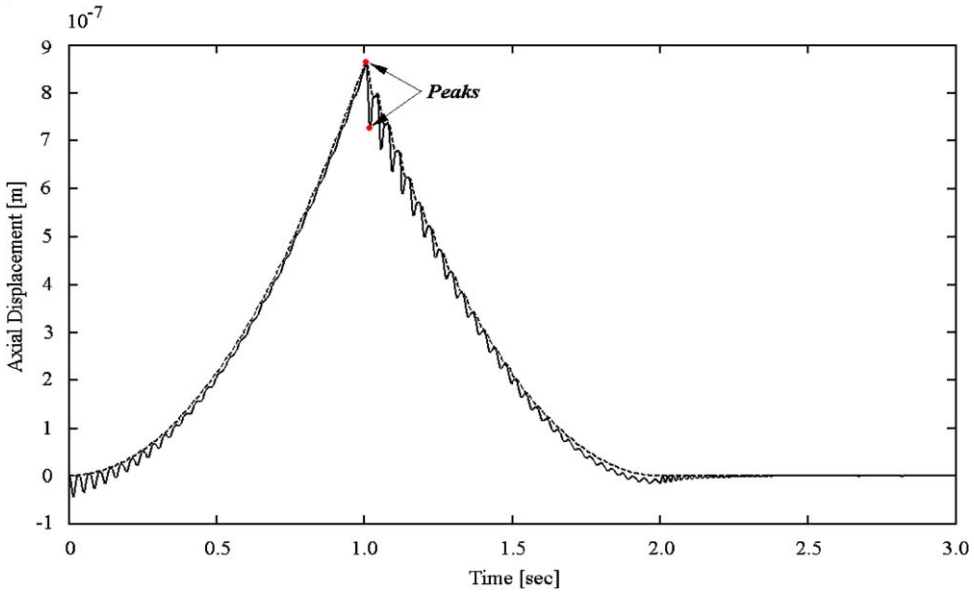

Fig. 7. Axial displacement for a beam rich in ceramic constituent, dotted line for linear approach and continuous line for nonlinear approach.

error in percentage (not shown in this paper due to space limitations) of the linear model with respect to the nonlinear model oscillates between 0.1 percent and 5 percent. On the other hand, for a metallic-rich beam, the same behavior of the ceramic-rich beam can be seen in Fig. 6; however, the error in percentage of the linear model with respect to the nonlinear model oscillates between 0.5 percent and 7 percent.

The differences between a linear and nonlinear formulation, and the influence of the geometrical stiffening can be exemplified in a more evident form by analyzing the dynamic behavior of the axial displacement. Since in the linear approach there is no elastic coupling between the lateral and axial displacement, the axial displacement is not influenced by the transient motion of the lateral displacement. This behavior can be seen in both Figs. 7 and 8. On the contrary the nonlinear approach has a coupling between lateral and axial displacements. Thus, the presence of a transient lateral motion induces by means of the geometrical coupling an axial displacement as one can see in the behavior of the nonlinear model in Figs. 7 and 8. The material properties as well as the type of formulation (linear or nonlinear) play an important role in the dynamics of functionally graded beams. This affirmation may be exemplified in Figs. 7 and 8. That is, the linear approach has no transient oscillatory motion, but the nonlinear approach has oscillatory motion. The intensity of this oscillatory

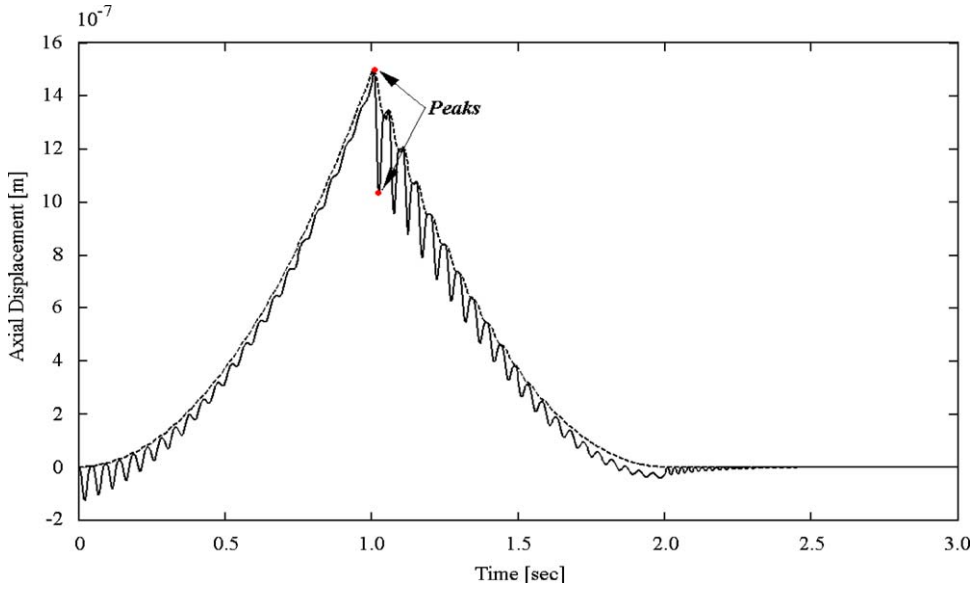

Fig. 8. Axial displacement for a beam rich in metallic constituent, dotted line for linear approach and continuous line for nonlinear approach.

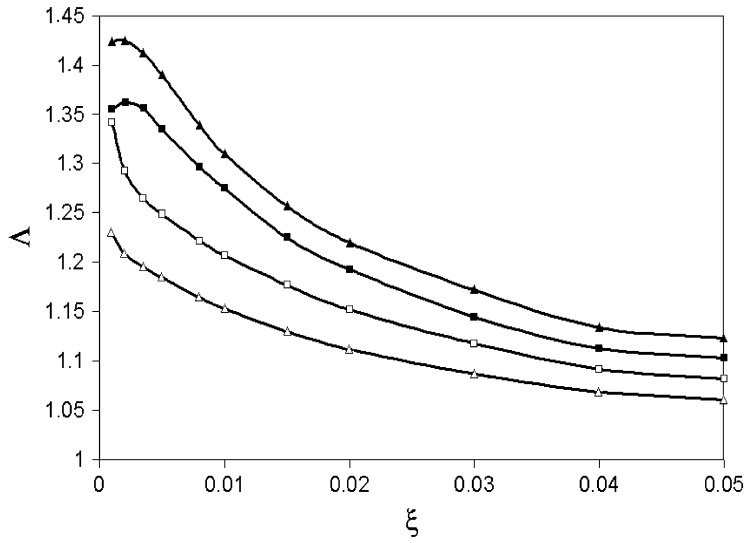

Fig. 9. Variation of the ratio Λ between transient peaks, (▲) for $n = 2.0$, (■) for $n = 1.5$, (□) for $n = 0.8$, (△) for $n = 0.4$.

motion, especially the peaks around $t = 1$ s, is related to the type of material properties. Thus, observing Figs. 7 and 8, it may be concluded that the aforementioned feature is connected with the presence of a higher content of metallic constituent in the beam. Note that in the case of the ceramic-rich beam ($n = 0.4$) the ratio between the indicated peaks is about 1.18 but in the case of a metallic-rich beam ($n = 2.0$) the ratio between the indicated peaks is of 1.43. In Fig. 9 one can see the variation of the aforementioned ratio between peaks (Λ) with respect to the damping coefficients ξ_i, which are assumed equal for comparative purposes among different types of metallic–ceramic ratios.

Taking into account that the axial stresses are related to the values of displacements through the constitutive equations, important changes in the forcing magnitude or sudden changes in the axial displacements would affect the stress patterns that may lead to undesired high stress levels, and eventually to a structural failure. A deeper analysis of this matter deserves a future work.

5. Conclusions

In this paper a new model to study the dynamic behavior of rotating beams made of functionally graded materials has been introduced. The model has been deduced employing a formulation accounting for shear-deformability and nonlinear

strain–displacements relationships. This conception makes possible the modeling of the geometric stiffening effect. The Coriolis inertial effect has been taken into account as well. The present model reproduces the results of other approaches based on Bernoulli–Euler assumptions and for isotropic materials. Certain features in the dynamics of rotating functionally graded beams have been evaluated through a couple of examples with a prescribed rule of rotation. In these tasks, the nonlinear approach and a derived linear approach have been compared. The ratio between constituents plays an important role in the dynamic behavior of the functionally graded beam. This is especially true if a certain beam is composed mainly of a metallic constituent, where in the case of rotating rules with sudden changes of acceleration, the axial displacement, for example, suffers a highly oscillatory behavior that may lead to a serious oscillatory pattern of axial stresses. However, this subject deserves a future and deeper research.

Acknowledgments

The support of Conselho Nacional de Pesquisa (CNPq) of Brasil, Faperj, Universidad Tecnológica Nacional and Consejo Nacional de Investigaciones Científicas y Tecnológicas (CONICET) of Argentina is kindly recognized.

References

[1] B.V. Sankar, An elasticity solution for functionally graded beams, *Composite Science and Technology* 61 (5) (2001) 689–696.
[2] A. Chakraborty, S. Gopalakrishnan, J.N. Reddy, A new beam finite element for the analysis of functionally graded materials, *International Journal of Mechanical Sciences* 45 (2003) 519–539.
[3] S. Kapuria, M. Bhattacharyya, A.N. Kumar, Bending and free vibration response of layered functionally graded beams: a theoretical model and its experimental validation, *Composite Structures* 82 (3) (2008) 390–402.
[4] J.S. Rao, Turbomachine blade vibration, *The Shock and Vibration Digest* 19 (1987) 3–10.
[5] J. Chung, H.H. Yoo, Dynamic analysis of a rotating cantilever beam using the finite element method, *Journal of Sound and Vibration* 249 (2002) 147–164.
[6] J. Simo, L. Vu-Quoc, A three dimensional finite-strain rod model. Part II, *Computer Methods in Applied Mechanics and Engineering* 58 (1986) 79–116.
[7] J. Simo, L. Vu-Quoc, The role of non-linear theories in transient dynamic analysis of flexible structures, *Journal of Sound and Vibration* 119 (3) (1987) 487–508.
[8] S.A. Fazelzadeh, P. Malekzaedh, P. Zahedinejad, M. Hosseini, Vibration analysis of functionally graded thin-walled rotating blades under high temperature supersonic flow using the differential quadrature method, *Journal of Sound and Vibration* 306 (2007) 333–348.
[9] S.A. Fazelzadeh, M. Hosseini, Aerothermoelastic behavior of supersonic rotating thin-walled beams made of functionally graded materials, *Journal of Fluids and Structures* 23 (2007) 1251–1264.
[10] M.A. Trindade, R. Sampaio, Dynamics of beams undergoing large rotations accounting for arbitrary axial deformation, *Journal of Guidance, Control and Dynamics* 25 (2002) 634–643.
[11] J.M. Mayo, D. Garcia-Vallejo, J. Domínguez, Study of the geometric stiffening effect: comparison of different formulations, *Multibody System Dynamics* 11 (2004) 321–341.
[12] E. Oñate, *Structural calculation with finite elements*, CIMNE, Barcelona, Spain, 1992 (in Spanish).
[13] J.S. Przemieniecki, *Theory of Matrix Structural Analysis*, McGraw-Hill Company, New York, 1968.
[14] K.J. Bathe, *Finite Element Procedures in Engineering Analysis*, Prentice-Hall, Englewood Cliffs, NJ, 1982.
[15] L. Meirovitch, *Principles and Techniques of Vibrations*, Prentice-Hall, Upper Saddle River, NJ, 1997.
[16] W. Carnegie, B. Dawson, Vibration characteristics of straight blades of asymmetrical aerofoil cross-section, *Aeronautical Quarterly* May (1963) 178.